Controls on the Activation and Strength of a High-Latitude Convective Cloud Feedback

Citation

Published Version

Permanent link

Terms of Use

Share Your Story

Controls on the Activation and Strength of a High-Latitude Convective Cloud Feedback

DORIAN S. ABBOT*† AND ELI TZIPERMAN ‡§

Harvard University, Cambridge, Massachusetts

Revised XX July 2008

*School of Engineering and Applied Sciences, Harvard University, Cambridge, MA 02138

†*Corresponding author address:* Dorian Abbot, Harvard University, 24 Oxford St, Cambridge, MA 02138. E-mail: abbot@fas.harvard.edu.

‡School of Engineering and Applied Sciences, Harvard University, Cambridge, MA 02138

§Department of Earth and Planetary Science, Harvard University, Cambridge, MA 02138

Abstract

Previous work has shown that a convective cloud feedback can greatly increase high-latitude surface temperature upon the removal of sea ice and can keep sea ice from forming throughout polar night. This feedback activates at increased greenhouse gas concentrations. It may help to explain the warm "equable climates" of the late Cretaceous and early Paleogene ($\sim$100-$\sim$35 million years ago) and may be relevant for future climate under global warming. Here the factors that determine the critical threshold CO_2 concentration at which this feedback is active and the magnitude of the warming caused by the feedback are analyzed using both a highly idealized model and NCAR's single column model (SCAM) run under Arctic-like conditions. The critical CO_2 is particularly important because it helps to establish the relevance of the feedback for past and future climates.

Both models agree that, in general, increased heat flux into the high latitudes at low altitudes decreases the critical CO_2. Increases in oceanic heat transport and in solar radiation absorbed during the summer should cause a sharp decrease in the critical CO_2, but the effect of increases in atmospheric heat transport depends on its vertical distribution. It is furthermore found that (1) if the onset of convection produces more clouds and moisture, the critical CO_2 should decrease and the maximum temperature increase caused by the convective cloud feedback should increase; (2) reducing the depth of convection reduces the critical CO_2 but has little effect on the maximum temperature increase caused by the convective cloud feedback. These results should help with interpretation of the strength and onset of the convective cloud feedback as found, for example, in IPCC coupled ocean-atmosphere models with different cloud and convection schemes.

1. Introduction

Cloud feedbacks represent the most important source of uncertainty in the climate system (Cess and co authors, 1990, 1996; Baker, 1997; Murphy et al., 2004; Stainforth et al., 2005; Soden and Held, 2006). This motivates the idea that cloud feedbacks might play an important role in explaining past "equable climates" and makes understanding clouds important for understanding future climate under increased greenhouse gas levels. Equable climates, which prevailed during the late Cretaceous and early Paleogene ($\sim$100 to $\sim$35 million years ago), were characterized by warm high latitudes (e.g., Zachos et al., 2001; Sluijs and coauthors, 2006), particularly during the winter and over continents (e.g., Greenwood and Wing, 1995), and tropical temperatures only somewhat higher than modern (e.g., Pearson et al., 2001; Norris et al., 2002; Roche et al., 2006; Tripati et al., 2003). Various mechanisms have been proposed to explain either the relatively cool tropical temperatures or relatively warm polar temperatures, including increased ocean heat transport due to ocean mixing by increased hurricane activity (Emanuel, 2002; Korty et al., 2008), the Hadley cell extending nearly to the pole (Farrell, 1990), and high-latitude longwave heating due to thick polar stratospheric clouds (Sloan et al., 1992; Sloan and Pollard, 1998; Peters and Sloan, 2000; Kirk-Davidoff et al., 2002).

Abbot and Tziperman (2008a) proposed a positive feedback on high-latitude temperatures that results from the onset of convective clouds. A related suggestion was also briefly made by Sloan et al. (1999) and Huber and Sloan (1999). In this proposed feedback, an initial warming leads to destabilization of the high-latitude atmosphere to convection, causing convection, which results in convective clouds and increased atmospheric moisture, both of which trap outgoing longwave radiation and lead to further warming.

Over ocean this feedback should occur preferentially during winter (Abbot and Tziperman, 2008b; Abbot et al., 2008) because during summer marine boundary layer clouds block low-level

atmospheric solar absorption so that solar absorption occurs preferentially in the mid-troposphere and stabilizes the lower atmosphere.

The convective cloud feedback as outlined in Abbot and Tziperman (2008b) and Abbot et al. (2008) is intimately tied to sea ice, which insulates the ocean and prevents convection when it is present, while the feedback prevents the formation of sea ice when there is none (Abbot and Tziperman, 2008b; Abbot et al., 2008). Abbot and Tziperman (2008a), however, found that the convective cloud feedback can operate based on atmospheric processes alone. This distinction is important because it underscores the possibility that the convective cloud feedback could lead to further warming even after the complete removal of sea ice and we will return to it in the discussion (section 4).

The convective cloud feedback allows for multiple equilibria: one solution which is convecting and is warm and another solution which is not convecting and is cold. The purpose of this paper is to determine what parameters control the lowest (critical) CO_2 value at which the warm state can exist and the temperature difference between the two states. The critical CO_2 is important because it determines whether the convective cloud feedback could have been active during periods of equable climate and whether it could be active in a future climate under global warming. The temperature difference between the two states is important because it represents the strength of the convective cloud feedback.

In section 2 we develop a simple two-level atmosphere-surface model that encapsulates the most basic physics that can describe the atmosphere-only convective cloud feedback. We use this model to qualitatively determine the way in which various parameters affect the onset of the feedback and its strength. This analysis should aid interpretation of the convective cloud feedback in more complex models, for example the IPCC coupled GCMs in which the convective cloud feedback has been shown to be active (Abbot et al., 2008).

In Section 3 we extend this analysis using SCAM, the NCAR single column atmospheric model. SCAM contains the full cloud, convection, and radiation parameterizations of the NCAR community atmosphere model (CAM), but heat transports into it and velocities acting on it must be prescribed. We show that SCAM's behavior is consistent with that of the two-level model and that the lessons from the simpler model can be used to understand the more complete SCAM.

2. Two-Level Model

a. Developing the Model

In this section we construct a simple two-level model of the atmosphere in which we attempt to capture the simplest system in which the convective cloud feedback can function. Based on previous work (Abbot and Tziperman, 2008a,b; Abbot et al., 2008) we expect the convective cloud feedback to be active at high latitudes (roughly poleward of 60°) during winter, and we will make assumptions accordingly throughout this section. In this model the top level represents the free troposphere (200-900 mb) (henceforth the atmosphere) and the lower level (henceforth the surface) represents the combined boundary layer (900-1000 mb) and surface, for example, a mixed-layer ocean (top 50 m). In effect we assume that turbulent fluxes tie the surface to the boundary layer so tightly that they behave as one. Energy balance for this model can be written

$$C_s \frac{dT_s}{dt} = F_s - F_c + \varepsilon\sigma T_a^4 - \sigma T_s^4, \tag{1}$$

$$C_a \frac{dT_a}{dt} = F_a + F_c + \varepsilon\sigma(T_s^4 - 2T_a^4). \tag{2}$$

Here C_s and C_a are the total heat capacities of the surface and atmospheric columns (standard heat capacity multiplied by total column mass), respectively; T_s and T_a are the surface and atmospheric temperatures, respectively; F_s is the heat flux into the surface and boundary layer from solar radi-

3

ation and by horizontal heat transport, which can be written $F_s = F_o + S(1-\alpha) + F_a^{bl}$ where F_o is the meridional ocean heat transport convergence, S is the solar heat flux, α is the albedo, and F_a^{bl} is the atmospheric transport convergence into the boundary layer; F_a is the meridional heat transport convergence into the atmospheric layer; F_c is the convective heat flux from the boundary layer to the free troposphere; ε is the emissivity of the free troposphere; and σ is the Stefan-Boltzmann constant.

The convective heat flux, F_c, and the free tropospheric emissivity, ε, depend on whether or not there is convection, which in turn depends on the moist stability. We determine moist stability by comparing the surface moist static energy (M_s)

$$M_s = C_p T_s + L r_s,$$

with the atmospheric saturation moist static energy (M_a^*)

$$M_a^* = C_p T_a + L r_a^* + g z_a,$$

where C_p is the specific heat of air at constant pressure, L is the latent heat of evaporation, r_s is the surface specific humidity, r_a^* is the free tropospheric saturation specific humidity, g is Earth's gravitational constant, and z_a is the height of the atmospheric layer (we specify the pressure of this layer, P_a, and calculate z_a using a scale height of 8 km). We calculate r_s by assuming a constant boundary layer relative humidity, RH. If $M_s < M_a^*$, the model is stable to moist convection and there is no convection, consequently we set the convective heat flux to zero $(F_c = 0)$ and we set the emissivity to a background value $(\varepsilon = \varepsilon_0)$. ε_0 represents the free tropospheric emissivity in the absence of convection, which should be roughly linear in $\log(CO_2)$ (Sasamori, 1968). Otherwise we choose F_c to satisfy the moist stability criticality $(M_s = M_a^*$, see below) and set $\varepsilon = \varepsilon_0 + \Delta\varepsilon$.

Our use of F_c to satisfy the moist stability criticality represents the basic physics of adjustment to a neutrally buoyant profile in a moist atmosphere. Our assumption that the atmospheric emissivity increases from a background emissivity (ε_0) when there is no convection by some offset ($\Delta\varepsilon$) upon the onset of convection represents the advent of radiatively thick convective clouds and the increase in high-altitude moisture; this is how the convective cloud feedback manifests itself in this model. Convective clouds could also affect the model albedo and through it F_s, however, based on previous SCAM and GCM investigations of the seasonality of the convective cloud feedback (Abbot and Tziperman, 2008b; Abbot et al., 2008), we will focus on high-latitude winters when the incoming solar radiation, S, is small or zero, making such an effect irrelevant.

We can solve for the steady-state solutions of the model by setting the time tendencies of (1-2) to zero. First consider the nonconvecting state, in which $F_c = 0$ and $\varepsilon = \varepsilon_0$. We have

$$0 = F_s + \varepsilon_0 \sigma T_{a1}^4 - \sigma T_{s1}^4, \tag{3}$$

$$0 = F_a + \varepsilon_0 \sigma (T_{s1}^4 - 2T_{a1}^4), \tag{4}$$

where the subscript 1 signifies that this is the nonconvecting solution. We can can solve (3-4) for the nonconvecting surface and atmospheric temperatures

$$T_{s1} = \left(\frac{2F_s + F_a}{(2 - \varepsilon_0)\sigma} \right)^{\frac{1}{4}} \tag{5}$$

$$T_{a1} = \left(\frac{\varepsilon_0 F_s + F_a}{(2 - \varepsilon_0)\varepsilon_0 \sigma} \right)^{\frac{1}{4}} \tag{6}$$

This solution is valid so long as $M_{s1} \leq M_{a1}^*$.

When the model is convecting, we obtain the equations

$$0 = F_s - F_c + \tilde{\varepsilon}\sigma T_{a2}^4 - \sigma T_{s2}^4, \tag{7}$$

$$0 = F_a + F_c + \tilde{\varepsilon}\sigma(T_{s2}^4 - 2T_{a2}^4), \tag{8}$$

$$C_p T_{s2} + L r_{s2} = C_p T_{a2} + L r_{a2}^* + g z_a \tag{9}$$

where $\tilde{\varepsilon} \equiv \varepsilon_0 + \Delta\varepsilon$ and the subscript 2 signifies the convecting solution. (9) represents the moist convective criticality ($M_{s2} = M_{a2}^*$). (7-9) can be solved for T_{s2}, T_{a2}, and F_c. This solution is valid so long as $F_c > 0$.

We plot the convecting and nonconvecting solutions of the two-level model as a function of ε_0 in Fig. 1. Here we choose F_a=100 W m^{-2}, which is a reasonable high-latitude value (Trenberth and Stepaniak, 2003), and F_s=250 W m^{-2}, which we take, for the most part, to represent heat absorbed and stored by the ocean during the summer and released back into the atmosphere during the winter. The simplicity of the model, with only one layer to represent the atmosphere, requires us to choose an unrealistically high F_s=250 W m^{-2} to achieve above-freezing surface temperatures. F_s takes much smaller values when we use the more realistic SCAM model (section 3). We take $\Delta\varepsilon$=0.3 and P_a=600 mb, representing medium-height convection that produces optically thick clouds.

The nonconvecting solution exists at all values of the clear-sky emissivity (ε_0) for these parameter choices (solid black line, Fig. 1a). For many other parameter choices, however, the nonconvecting solution does not exist at high ε_0. The convecting solution exists at high ε_0, but disappears for ε_0 below some critical ε_0 which we call ε_c. ε_c is the two-level model analogue of the logarithm of the critical CO$_2$. Below ε_c, the two-level model is no longer warm enough to consistently sustain convection (that is, (7-9) yield $F_c < 0$). Because the free tropospheric emissivity is increased by $\Delta\varepsilon$ due to the appearance of convective clouds and increased moisture in the convecting solution,

6

the convecting solution has a higher surface temperature than the nonconvecting solution at all ε_0.

The vertical temperature profile of the convecting solution follows the moist lapse rate, whereas the lapse rate of the nonconvecting solution is determined radiatively (Fig. 1d). This causes the nonconvecting surface temperature to increase much faster with ε_0 than the convecting surface temperature does ($\frac{dT_{s1}}{d\varepsilon_0} > \frac{dT_{s2}}{d\varepsilon_0}$, Fig. 1a). Consequently, the maximum difference in surface temperature between the convecting and nonconvecting solutions as a function of ε_0, $(T_{s2} - T_{s1})_{max}$, occurs at the minimum value of ε_0 at which convection is possible ($\varepsilon_0 = \varepsilon_c$).

There is a singularity in the nonconvecting atmospheric temperature (6) as ε_0 approaches zero if F_a, the atmospheric heat transport, is nonzero. This leads to a negative lapse rate at low ε_0 (Fig. 1(d)), which to some extent could be a realistic representation of a high-latitude winter inversion; however, the extreme increase of T_{a1} as ε_0 goes to zero is due to the simplicity of the model and is not realistic. In any case, this does not affect the surface temperature (5), which is the quantity in which we are primarily interested.

b. Using the Model to Understand the Convective Cloud Feedback

We now focus on how the model parameters affect ε_c, the lowest ε_0 at which the convecting solution can exist, and $(T_{s2} - T_{s1})_{max}$, the maximum difference in surface temperature between the convecting and nonconvecting solutions as a function of ε_0. ε_c is important for two reasons. First, since ε_0 can be thought of as roughly representing $\log(CO_2)$ in this model, ε_c is related to the lowest CO_2 concentration at which the convecting solution can exist, which is critical to whether or not the convecting solution could be realized during an equable climate or future climate with increased greenhouse gases. Second, as $(T_{s2} - T_{s1})_{max}$ occurs at $\varepsilon_0 = \varepsilon_c$ and $\frac{dT_{s1}}{d\varepsilon_0} > \frac{dT_{s2}}{d\varepsilon_0}$, decreasing ε_c tends to increase $(T_{s2} - T_{s1})_{max}$, which is itself important because $(T_{s2} - T_{s1})_{max}$ represents the strength of the convective cloud feedback. Stated again, the lower the critical CO_2, the larger the

maximum temperature increase caused by the convective cloud feedback, all other things being equal.

In Figs. 2-3, we show how $(T_{s2} - T_{s1})_{max}$ and ε_c change as we vary $\Delta\varepsilon$, F_s, F_a, and P_a, which are the important independent model parameters. $\Delta\varepsilon$ represents the increase in optical thickness of the atmosphere associated with clouds and water vapor upon the onset of convection. We see F_s as mostly representing solar heat absorbed by the surface during summer and released into the atmosphere during the winter. F_a represents the convergence of atmospheric heat transport. P_a represents the depth of convection. Our main findings in this section are that changing $\Delta\varepsilon$ has a significant effect on $(T_{s2} - T_{s1})_{max}$ whereas changing the other variables does not, and that ε_c tends to be more sensitive to changes in all the variables than $(T_{s2} - T_{s1})_{max}$ does.

Increasing $\Delta\varepsilon$ causes no change in the nonconvecting solution. Increasing $\Delta\varepsilon$ warms the convecting solution, which itself increases $(T_{s2} - T_{s1})_{max}$, but it also allows the convecting solution to exist at lower ε_0 (Fig. 3a), which, as explained above, further increases $(T_{s2} - T_{s1})_{max}$ (Fig. 2a).

Increasing F_s, which destabilizes the atmosphere to convection, allows the convecting solution to exist at lower ε_0 (decreases ε_c, Fig. 3b); however, $(T_{s2} - T_{s1})_{max}$ increases slightly as F_s increases (Fig. 2b) instead of decreasing as one might expect from the decrease in ε_c. This is because the surface and atmosphere are more tightly coupled in the convecting solution so more of the heating resulting from increasing F_s goes into increasing the surface temperature in the nonconvecting solution than in the convecting solution.

Increasing F_a increases the surface temperature more in the convecting solution than in the nonconvecting solution, which increases $(T_{s2} - T_{s1})_{max}$ (Fig. 2c), because the surface and atmosphere are more tightly coupled in the convecting solution. The warming effect of F_a tends to destabilize the atmosphere to convection, but this effect is dominated by the direct stabilizing effect of F_a so that ε_c increases with F_a (Fig. 3c). This increase in ε_c as F_a increases helps to explain why the

8

increase in $(T_{s2} - T_{s1})_{max}$ with F_a is so small.

Increasing P_a has no effect on the nonconvecting solution. It does cause a large decrease in ε_c (Fig. 3d) because it is easier to reach the moist convective criticality if the height of convection is lower (the gravitational term in (9) is smaller). Decreasing the height of convection also means that the T_{a2} is closer to T_{s2}, so that the atmosphere provides less radiative forcing, and $(T_{s2} - T_{s1})_{max}$ decreases somewhat as P_a is increased. This effect is relatively large at any particular value of ε_0, but the effect on the maximum temperature difference is muted by the fact that ε_c decreases as well as P_a is increased.

3. SCAM

We next analyze SCAM to determine whether the insight provided by the simple analytical model regarding the critical CO_2 needed for the warm convecting state to exist (ε_c) and the maximum strength of the convective cloud feedback ($(T_{s2} - T_{s1})_{max}$) is valid in a more quantitative model. As in section 2 we are interested in investigating the convective cloud feedback in SCAM at high latitudes and during winter. Consequently we run SCAM to steady state in simulated polar night (zero solar forcing, S=0). The real Arctic ocean is not in steady state during polar night: it radiates heat to space throughout polar night and continually cools. We have, however, already shown that the convective cloud feedback can function in the presence of a seasonal cycle (Abbot and Tziperman, 2008b; Abbot et al., 2008), and, as our objective here is to understand the feedback in depth, we feel justified in using the steady state assumption, which greatly simplifies our analysis. In addition, in an ice-free Arctic ocean, the surface heat capacity would be very high so that the approximation of considering the steady state solution should be reasonable. In order to obtain an above-freezing equilibrated surface temperature at realistic atmospheric heat transport (AHT) values, we need to specify a nonzero net surface heat flux (NSHF) from the surface to the atmo-

sphere. The NSHF represents a combination of the convergence of ocean heat transport and the winter release of heat that the ocean stored during the summer.

We couple SCAM to a mixed layer ocean of depth 50 m, set the surface wind velocity to a constant 5 m s^{-1}, and set the vertical velocity to zero at all vertical levels. We run SCAM with ozone and sea salt aerosol set to their annual mean values at a latitude of 79.5°N and a longitude of 143.4°W, which is over the Arctic Ocean. We set all other aerosol concentrations to zero. All boundary conditions that we apply to SCAM are time-invariant. We apply the AHT to the atmosphere as dry transport equally by mass below 200 mb, with the AHT going to zero smoothly as a hyperbolic tangent with a vertical thickness of 50 mb. This means that, other than the smoothing near 200 mb, the applied temperature tendency is the same for each pressure level below 200 mb. In a related study, Abbot and Tziperman (2008b) found that the apportionment of AHT between dry and moist transport did not qualitatively affect their results.

When we run SCAM with zero solar forcing (S=0) and large enough AHT and NSHF values, we find multiple equilibria, with a stable warm and convecting state possibly relevant to both future greenhouse warming and past equable climates, over a wide range of CO_2 values (e.g., Fig. 4-5). In Fig. 4 we show the surface temperature of the warm and cold states with a realistic polar AHT of 100 W m^{-2} and different NSHF values, while in Fig. 5 we show that both states exist even when we drastically change the distribution of heat transports to NSHF=170 W m^{-2} and AHT=0 W m^{-2}. The solution of SCAM (Fig. 4-5) as a function of log(CO_2) looks similar to that of the two-level model (Fig. 1) as a function ε_0. There is a wide range in log(CO_2) over which both the warm and cold solutions exist and, particularly in Fig. 5, the surface temperature of the cold state increases faster with CO_2 than the surface temperature of the warm state. The cold state sea surface temperature sometimes reaches the freezing point of seawater, -1.8°C, (Fig. 4) in which case we hold the sea surface temperature at this value. This represents an extra artificial heat flux

from the surface into the atmosphere, in addition to the applied NSHF, however, even with this extra heat flux the cold state is still stable. Such cold states would approach the ice-states of Abbot and Tziperman (2008b) if allowed to fully equilibrate in a model that included sea ice.

The warm equilibrium is significantly warmer than the cold equilibrium when both states exist. For example, with CO_2=2 000 ppm, AHT=100 W m^{-2}, and NSHF=70 W m^{-2}, the surface temperature is 7.0°C in the warm state and -1.8°C in the cold state (it is prescribed not to go below the freezing temperature of sea water, as described above). The convective cloud feedback is the major cause of this difference, as the cloud radiative forcing in the warm state (45.7 W m^{-2}) is nearly double that in the cold state (25.6 W m^{-2}). The change in cloud radiative forcing is due to more and thicker high clouds in the warm state (Fig. 6c,d). These clouds result from stronger and deeper convection (Fig. 6g,h), which leads to increased mid-tropospheric ice condensate (Fig. 6f) and increased cloud fraction (Fig. 6c).

SCAM calculates the depth of convection, thickness of clouds, and amount of moisture. So in SCAM there are no analogues to P_a and $\Delta\varepsilon$ from the two-level model for us to vary; however, we can investigate the effect of changing the NSHF (analogue of F_s in the two-level model) and the AHT (analogue of F_a, with a complication to be explained) on the convective cloud feedback in SCAM. The lowest CO_2 at which the warm state exists (critical CO_2, analogue of ε_c in the two-level model), one of the most important variables investigated in this paper, decreases sharply as the NSHF is increased (Table 1), which is consistent with the strong decrease of ε_c as F_s increases in the two-level model (Fig. 3b). For AHT values comparable to modern Arctic values, the critical CO_2 spans the entire plausible CO_2 range for the early Paleogene ($\sim$250-$\sim$4000 ppm, Pagani et al., 2005; Pearson and Palmer, 2000) when the NSHF is changed by 20 W m^{-2} (Table 1). This underscores the importance of the absorption of summer solar radiation for the maintenance of the warm state.

11

The critical CO_2 in SCAM also decreases sharply as the AHT is increased, which appears to contradict the increase in ε_c as F_a increases in the two-level model (Fig. 3c). The main reason for this is that, as the AHT in SCAM is applied equally throughout the troposphere, it is not a direct analogue for F_a from the two-level model, but should actually be thought of as some combination of F_s and F_a. Furthermore, an AHT applied in this way does not directly change the stability, so that its main effect is to warm the model, which decreases the critical CO_2. We should note that the formulation of the vertical distribution of AHT in SCAM we have used is not necessarily realistic, as, for example, we have not taken into account reduced near-surface AHT due to surface friction (e.g., Branscome et al., 1989; Stone and Yao, 1990). The main lesson we should learn from these SCAM runs and the two-level model is that the effect of the AHT on the critical CO_2 depends strongly on the detailed vertical distribution of AHT.

There is no discernible pattern in the change in the maximum surface temperature difference between the warm and cold states as AHT and NSHF are varied (Table 2). This is consistent with the relatively small changes in $(T_{s2} - T_{s1})_{max}$ as F_s and F_a are varied in the two-level model (section 2b). Additionally, because of the high sensitivity of the critical CO_2 to NSHF, we only vary AHT and NSHF over relatively small ranges compared to the ranges over which we varied F_s and F_a in the two-level model.

4. Discussion

Results from the two-level model (section 2) helped us motivate and understand results from SCAM (section 3). For example, both models agree that the critical CO_2 at which the convective cloud feedback activates is sharply dependent on surface heat flux. As far as the surface heat flux in these models can be interpreted as the winter release of heat stored by the ocean during the summer, this suggests that more clouds during summer, which reflect solar radiation and there-

fore reduce the amount of solar radiation absorbed by the surface, should lead to a higher critical CO_2. The use of both models in conjunction with each other also helped us understand that the vertical distribution of the atmospheric heat transport is at least as important as its magnitude for determining the critical CO_2. This represents an important limitation on our ability to predict the critical CO_2 since currently even the magnitude of the atmospheric heat transport during equable climates, resulting from a competition between reduced dry static energy transport, due to reduced meridional temperature gradient, and increased latent energy transport, due to increased subtropical temperature and moisture, is unknown (Pierrehumbert, 2002; Caballero and Langen, 2005).

The two-level model, however, is useful beyond its relation to SCAM. SCAM interactively predicts the depth of convection, thickness of clouds, and amount of moisture, whereas, in the two-level model we are able to vary these at will, through the parameters $\Delta\varepsilon$ and P_a, to understand their effect on the convective cloud feedback. The main interesting and unexpected results from the two-level model are that increasing the height of convection significantly increases the critical CO_2 and that increasing the height of convection has very little effect on the maximum surface temperature difference between the cold and warm state, although it does significantly increase the convecting solution surface temperature and, therefore, the surface temperature difference at any particular ε_0 (CO_2).

This type of understanding, gained from the two-level model, could be quite useful for interpretation of general circulation model (GCM) results. For example Abbot et al. (2008) found that the convective cloud feedback increased the uncertainty in winter sea ice forecasts in the coupled ocean-sea ice-land-atmosphere GCMs that participated in the IPCC fourth assessment report 1%/year CO_2 increase to quadrupling scenario. The extent to which sea ice was lost and the feedback was active are related to the critical CO_2 and perhaps insight from the two-level model could help us understand the differences between these models.

13

Two of the GCMs that participated in the IPCC fourth assessment report 1%/year CO_2 increase to quadrupling scenario completely lost winter sea ice at the end of the experiment. The Arctic winter sea surface temperature in these models was barely above freezing, and the cloud radiative forcing was about 30 W m^{-2} which, though significant, is much smaller than roughly 50 W m^{-2} found in SCAM in this paper and by Abbot and Tziperman (2008b) when the surface temperature was 10-15°C higher. This difference in cloud radiative forcing was mainly due to the fact that the convection was shallower in the ice-free GCMs (reaching about 800 mb) than in SCAM (reaching 400-500 mb). Abbot et al. (2008) speculated that the GCMs might have produced deeper convection and a stronger feedback if the CO_2 were further increased or the run were integrated until it were closer to equilibrium. This paper raises the possibility that the convective cloud feedback operating in the atmosphere alone could introduce sufficient nonlinearity to allow a hysteresis such that if the GCMs were started from much warmer ice-free conditions, instead of ice-covered conditions, they might have equilibrated with deeper convection and a higher surface temperature like SCAM did.

Renno (1997) and Sobel et al. (2007) have found multiple equilibria in single column atmospheric models that include representations of the hydrological cycle. The Renno (1997) study does not include clouds, so it is quite different from this study. The work of Sobel et al. (2007) is more similar to this study in that they find two separate steady-states, one convecting, and one not convecting; however, by using the weak temperature gradient assumption, they focus on the tropics, and their model uses fixed surface temperatures, rather than prognostic surface temperatures in an energy-conserving model. The convecting and nonconvecting states of Sobel et al. (2007) are not "warm" and "cold," since both are forced at the same surface temperature, rather they are "wet" and "dry."

In the two-level model of section 2, we assumed that the atmospheric emissivity increased

by a constant offset ($\Delta\varepsilon$) upon the onset of convection. One might alternatively suspect that the radiative effect of convective clouds might increase with the strength of convection. This is the case in the warm SCAM states of Fig. 4: the cloud radiative forcing increases roughly linearly with the maximum convective mass flux in the mid-troposphere (not shown). When we modify the two-level model so that the emissivity increases linearly with the convective heat flux (F_c) instead of all at once when convection starts, we find that the model still exhibits hysteresis and our main conclusions are unaltered.

The convective cloud feedback could help to keep the Arctic ocean ice-free throughout the winter. This would likely lead to a situation with relatively warm ocean surrounded by relatively cold continent. This could lead to a low pressure system over the ocean and possibly, even though the Coriolis parameter would be large and the Ekman number small, lead to Ekman pumping, inflow at low levels, and vertical ascent. In this paper, we have specified the vertical velocity to be zero at every level (section 3), so we have neglected such an effect; however, it seems likely that such upward motion would augment the convective activity over the ocean.

The two-level model we used in this study is intentionally quite simple and SCAM, though it has sophisticated cloud, convection, and radiation schemes, lacks dynamics. In both models we need to specify horizontal heat transports, which define the models' interaction with surrounding areas, and prescribe a net surface heat flux to simulate seasonal heat storage. In some sense the simplicity of these models is a limitation of this study; however, the convective cloud feedback has been shown to be active in state-of-the-art coupled GCMs (Abbot et al., 2008) and here we have used the two simple models in conjunction to gain a deeper understanding of the feedback.

A major part of the equable climate mystery is warmth during the winter in continental interiors (e.g., Greenwood and Wing, 1995). Implicitly, this paper has focused on polar night over oceans since we have net heat flux from the surface into the atmosphere, which would have to come from

15

either ocean heat transport or the storage of heat during the summer by the ocean and release during the winter. We are currently investigating the role the convective cloud feedback could play in warming continental interiors.

5. Conclusions

In this paper we used a simple two-level model of the atmosphere and ocean and NCAR's single column atmospheric model coupled to a mixed layer ocean to analyze the critical CO_2 concentration at which a high-latitude convective cloud feedback can become active and the strength of this high-latitude convective cloud feedback, as measured by its ability to raise the surface temperature. The critical CO_2 is particularly important because it determines whether the convective cloud feedback could have been active during periods of equable climate and in a future climate, because understanding what controls it may aide in understanding why the convective cloud feedback is more active in some GCMs than in others at the same CO_2 concentration, and because it has a large effect on the overall strength of the feedback (section 2b). Our main findings follow.

- If the feedback produces more and thicker convective clouds, it should activate at a lower CO_2 and be stronger.

- If the feedback produces deeper convection, it should activate at a higher CO_2, be much stronger at any particular CO_2, and have a somewhat larger maximum strength.

- If the net heat released by the surface during winter, produced either by ocean heat transport or by the release of seasonally-stored heat, increases, the critical CO_2 should decrease sharply and the strength of the feedback should not change much.

- The effects of atmospheric heat transport are complicated and depend on the detailed vertical structure of this heat transport.

16

REFERENCES

Abbot, D. S., and E. Tziperman, 2008a: A high-latitude convective cloud feedback and equable climates. *Q. J. R. Meteorol. Soc.*, **134**, DOI: 10.1002/qj.211.

Abbot, D. S., and E. Tziperman, 2008b: Sea ice, high-latitude convection, and equable climates. *Geophys. Res. Lett.*, **35**, L03,702, doi:10.1029/2007GL032,286.

Abbot, D. S., C. C. Walker, and E. Tziperman, 2008: Winter arctic sea ice uncertainty under global warming due to a cloud radiative feedback. Submitted, available at http://swell.eps.harvard.edu/~abbot/PAPERS/abbot-tziperman-08c.pdf.

Baker, M. B., 1997: Cloud microphysics and climate. *Science*, **276**(5315), 1072–1078.

Branscome, L. E., W. J. Gutowski, and D. A. Stewart, 1989: Effect of surface fluxes on the nonlinear development of baroclinic waves. *Journal of the Atmospheric Sciences*, **46**(4), 460–475.

Caballero, R., and P. L. Langen, 2005: The dynamic range of poleward energy transport in an atmospheric general circulation model. *Geophys. Res. Lett.*, **32**.

Cess, R. D., and co authors, 1990: Intercomparison and interpretation of cloud-climate feedback processes in 19 atmospheric general circulation models. *J. Geophys. Res.*, **95**, 16,601–16,615.

Cess, R. D., and co authors, 1996: Cloud feedback in atmospheric general circulation models: an update. *J. Geophys. Res.*, **101**, 12,791–94.

Emanuel, K., 2002: A simple model of multiple climate regimes. *J. Geophys. Res.*, **107**(0).

Farrell, B. F., 1990: Equable climate dynamics. *Journal of the Atmospheric Sciences*, **47**(24), 2986–2995.

Greenwood, D. R., and S. L. Wing, 1995: Eocene continental climates and latitudinal temperature gradients. *Geology*, **23**(11), 1044–1048.

Huber, M., and L. C. Sloan, 1999: Warm climate transitions: A general circulation modeling study of the Late Paleocene Thermal Maximum ($\sim$56 ma). *J. Geophys. Res.*, **104**, 16,633–16,655.

Kirk-Davidoff, D. B., D. P. Schrag, and J. G. Anderson, 2002: On the feedback of stratospheric clouds on polar climate. *Geophysical Research Letters*, **29**(11).

Korty, R. L., K. A. Emanuel, and J. R. Scott, 2008: Tropical cyclone mixing during equable climates: could enhanced ocean mixing weaken meridional temperature gradients? *J. Climate*, **21**, 638Ð654, doi:10.1175/2007JCLI1659.1.

Murphy, J. M., D. M. H. Sexton, D. N. Barnett, G. S. Jones, M. J. Webb, and M. Collins, 2004: Quantification of modelling uncertainties in a large ensemble of climate change simulations. *Nature*, **430**(7001), 768–772.

Norris, R. D., K. L. Bice, E. A. Magno, and P. A. Wilson, 2002: Jiggling the tropical thermostat in the Cretaceous hothouse. *Geology*, **30**(4), 299–302.

Pagani, M., J. C. Zachos, K. H. Freeman, B. Tipple, and S. Bohaty, 2005: Marked decline in atmospheric carbon dioxide concentrations during the Paleogene. *Science*, **309**, 600–603.

Pearson, P. N., and M. R. Palmer, 2000: Atmospheric carbon dioxide concentrations over the past 60 million years. *Nature*, **406**, 695–699.

Pearson, P. N., P. W. Ditchfield, J. Singano, K. G. Harcourt-brown, C. J. Nicholas, R. K. Olsson, N. J. Shackleton, and M. A. Hall, 2001: Warm tropical sea surface temperatures in the Late Cretaceous and Eocene epochs. *Nature*, **413**(6855), 481–487.

Peters, R. B., and L. C. Sloan, 2000: High concentrations of greenhouse gases and polar strato-spheric clouds: A possible solution to high-latitude faunal migration at the latest Paleocene thermal maximum. *Geology*, **28**(11), 979–982.

Pierrehumbert, R. T., 2002: The hydrologic cycle in deep-time climate problems. *Nature*, **419**(6903), 191–198.

Renno, N. O., 1997: Multiple equilibria in radiative-convective atmospheres. *Tellus Series a-dynamic Meteorology and Oceanography*, **49**(4), 423–438.

Roche, D. M., Y. Donnadieu, E. Puceat, and D. Paillard, 2006: Effect of changes in delta o-18 content of the surface ocean on estimated sea surface temperatures in past warm climate. *Paleoceanography*, **21**(2).

Sasamori, T., 1968: The radiative cooling calculation for application to general circulation ex-periments. *J. Appl. Meteor.*, **7**, 721–729.

Sloan, L. C., and D. Pollard, 1998: Polar stratospheric clouds: A high latitude warming mecha-nism in an ancient greenhouse world. *Geophysical Research Letters*, **25**(18), 3517–3520.

Sloan, L. C., J. C. G. Walker, T. C. Moore, D. K. Rea, and J. C. Zachos, 1992: Possible methane-induced polar warming in the early Eocene. *Nature*, **357**(6376), 320–322.

Sloan, L. C., M. Huber, and A. Ewing, 1999: Polar stratospheric cloud forcing in a greenhouse world: A climate modeling sensitivity study. *Reconstructing Ocean History: A Window into the Future*, F. Abrantes and A. Mix, Eds., Kluwer Academic / Plenum Publishers, pp. 273–293.

Sluijs, A., and coauthors, 2006: Subtropical Arctic ocean temperatures and Palaeocene/Eocene thermal maximum. *Nature*, **441**, 610–613.

Sobel, A. H., G. Bellon, and J. Bacmeister, 2007: Multiple equilibria in a single-column model of the tropical atmosphere. *Geophysical Research Letters*, **34**(22).

Soden, B. J., and I. M. Held, 2006: An assessment of climate feedbacks in coupled ocean-atmosphere models. *J. Climate*, **19**(14), 3354–3360.

Stainforth, D. A., et al., 2005: Uncertainty in predictions of the climate response to rising levels of greenhouse gases. *Nature*, **433**(7024), 403–406.

Stone, P. H., and M.-S. Yao, 1990: Development of a two-dimensional zonally averaged statistical-dynamical model. Part III: The parameterization of the eddy fluxes of heat and moisture. *J. Climate*, **3**, 726–740.

Trenberth, K. E., and D. P. Stepaniak, 2003: Covariability of components of poleward atmospheric energy transports on seasonal and interannual timescales. *J. Climate*, **16**, 3691–3705.

Tripati, A. K., M. L. Delaney, J. C. Zachos, L. D. Anderson, D. C. Kelly, and H. Elderfield, 2003: Tropical sea-surface temperature reconstruction for the early Paleogene using Mg/Ca ratios of planktonic foraminifera. *Paleoceanography*, **18**(4), 1–13.

Zachos, J., M. Pagani, L. Sloan, E. Thomas, and K. Billups, 2001: Trends, rhythms, and aberrations in global climate 65 Ma to present. *Science*, **292**(5517), 686–693.

List of Figures

FIGURE 1: Solution to the two-level model as a function of ε_0, which is a proxy for $\log(CO_2)$ concentration. (a) Nonconvecting solution surface temperature (T_{s1}, black solid line) and convecting solution surface temperature (T_{s2}, grey dashed line), (b) difference between the surface temperature of the convecting and nonconvecting solutions ($T_{s2} - T_{s1}$), (c) nonconvecting solution atmospheric temperature (T_{a1}, black solid line) and convecting solution atmospheric temperature (T_{a2}, grey dashed line), (d) nonconvecting solution lapse rate ($T_{s1} - T_{a1}$, black solid line) and convecting solution lapse rate ($T_{s2} - T_{a2}$, grey dashed line). Model parameters are: F_s=250 W m^{-2}, F_a=100 W m^{-2}, ε_0=0.5, $\Delta\varepsilon$=0.3, P_a=600 mb, and RH=0.85.
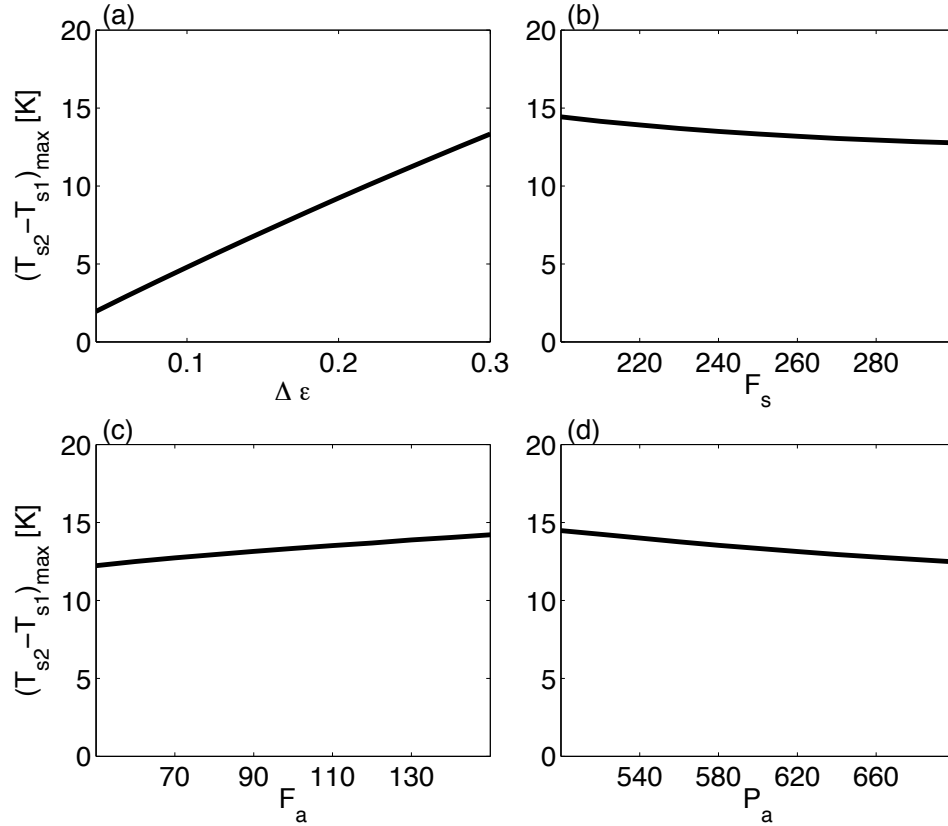
FIGURE 2: Maximum difference in surface temperature between the convecting and nonconvecting solutions as a function of (a) $\Delta\varepsilon$, the increase in atmospheric emissivity resulting from the onset of convection; (b) F_s, the heat flux into the surface, we view as mostly representing solar heat absorbed by the surface during summer and released into the atmosphere during the winter; (c) F_a, the heat flux into the atmosphere; (d) P_a, pressure of the atmospheric level (depth of convection). Model parameters, except the parameter varied, are as in Fig. 1.
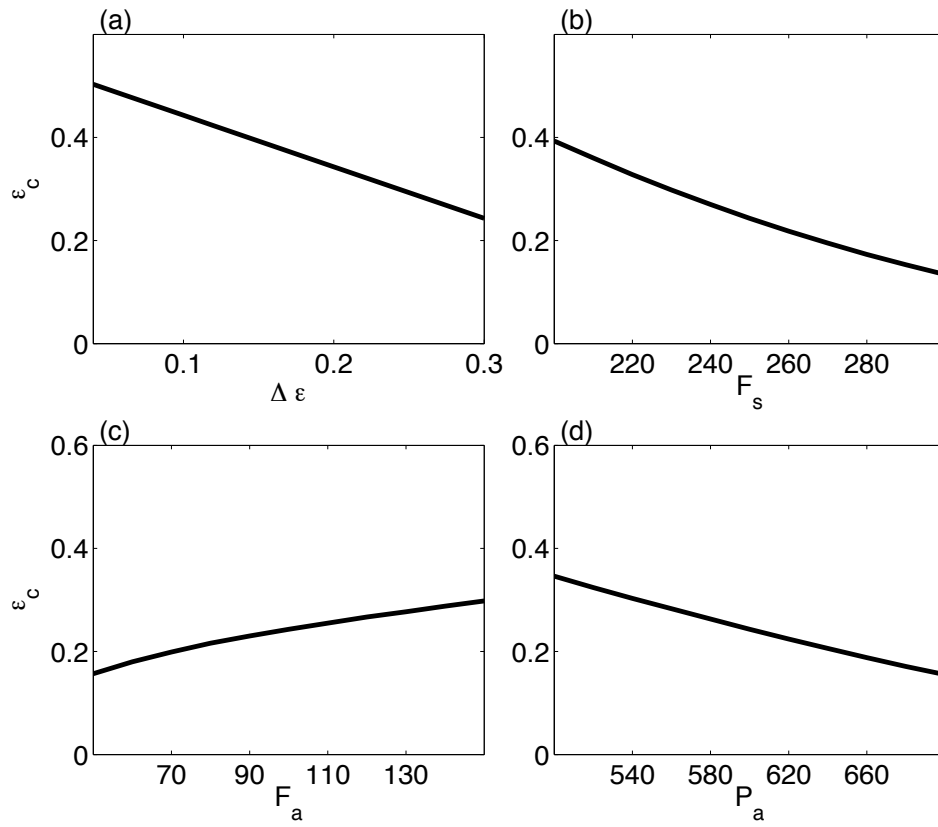
FIGURE 3: As in Fig. 2, but for ε_c, the smallest emissivity at which the convective solution exists.
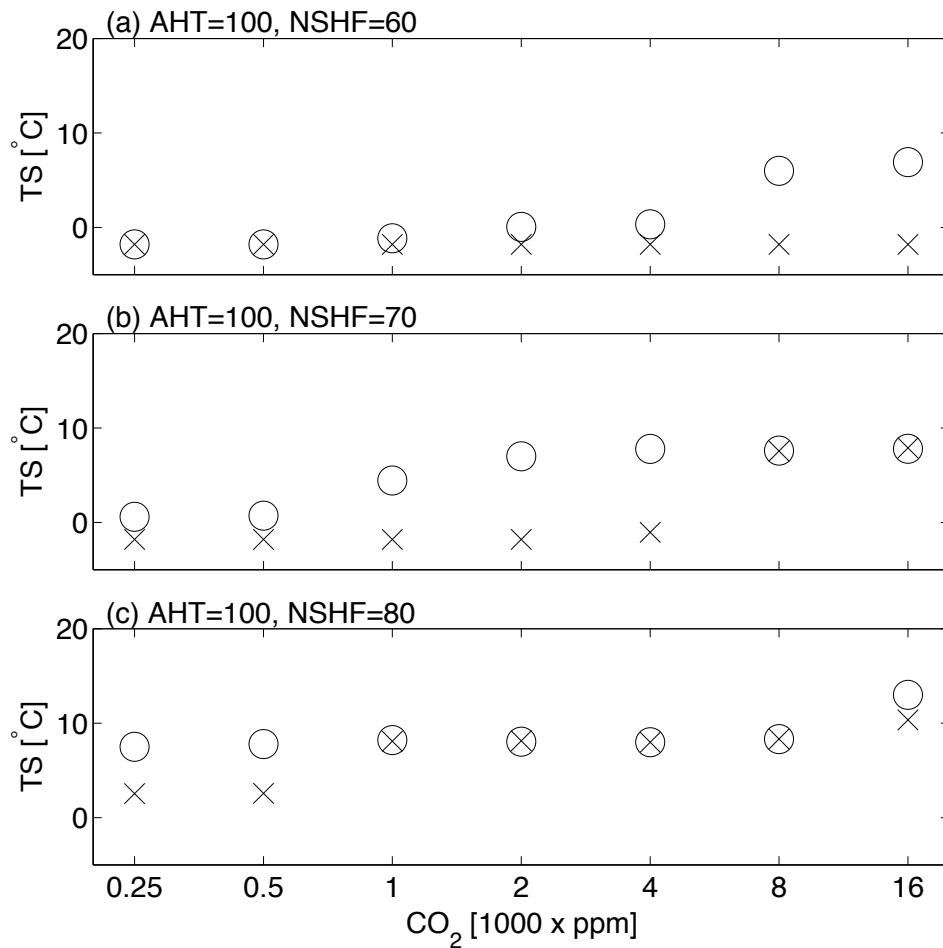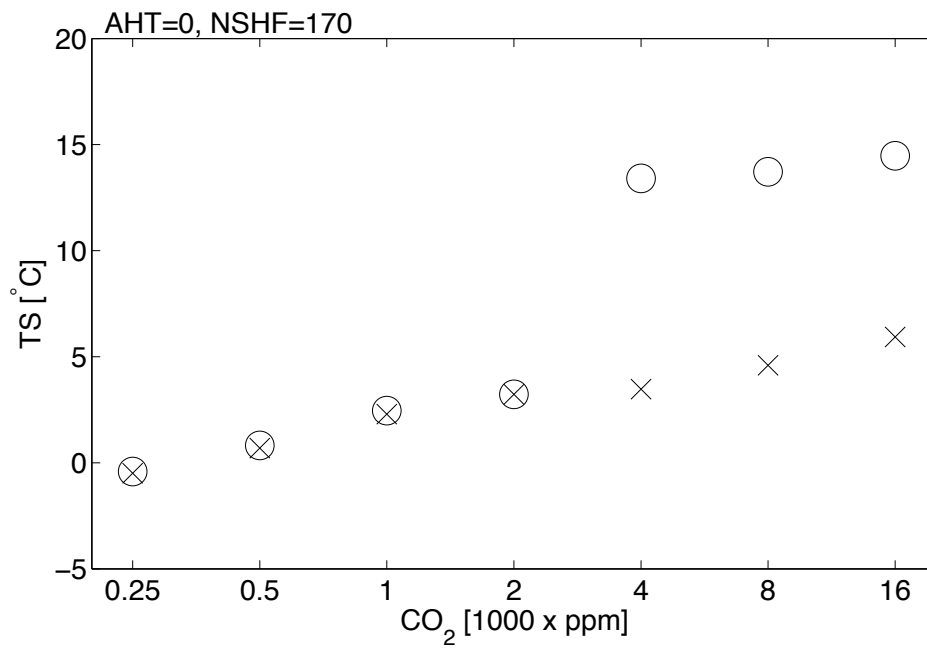
FIGURE 4: Equilibrated surface temperature (TS) of the warm (circles) and cold (crosses) states in SCAM at different CO_2 levels with zero solar radiation ($S=0$ W m^{-2}), an atmospheric heat transport (AHT) of 100 W m^{-2}, and a net surface heat flux (NSHF) of (a) 60 W m^{-2}, (b) 70 W m^{-2}, (c) 80 W m^{-2}.

FIGURE 5: Equilibrated surface temperature (TS) of the warm (circles) and cold (crosses) states in SCAM at different CO_2 levels with zero solar radiation (S=0 W m^{-2}), zero atmospheric heat transport (AHT=0 W m^{-2}), and a net surface heat flux (NSHF) of 170 W m^{-2}.
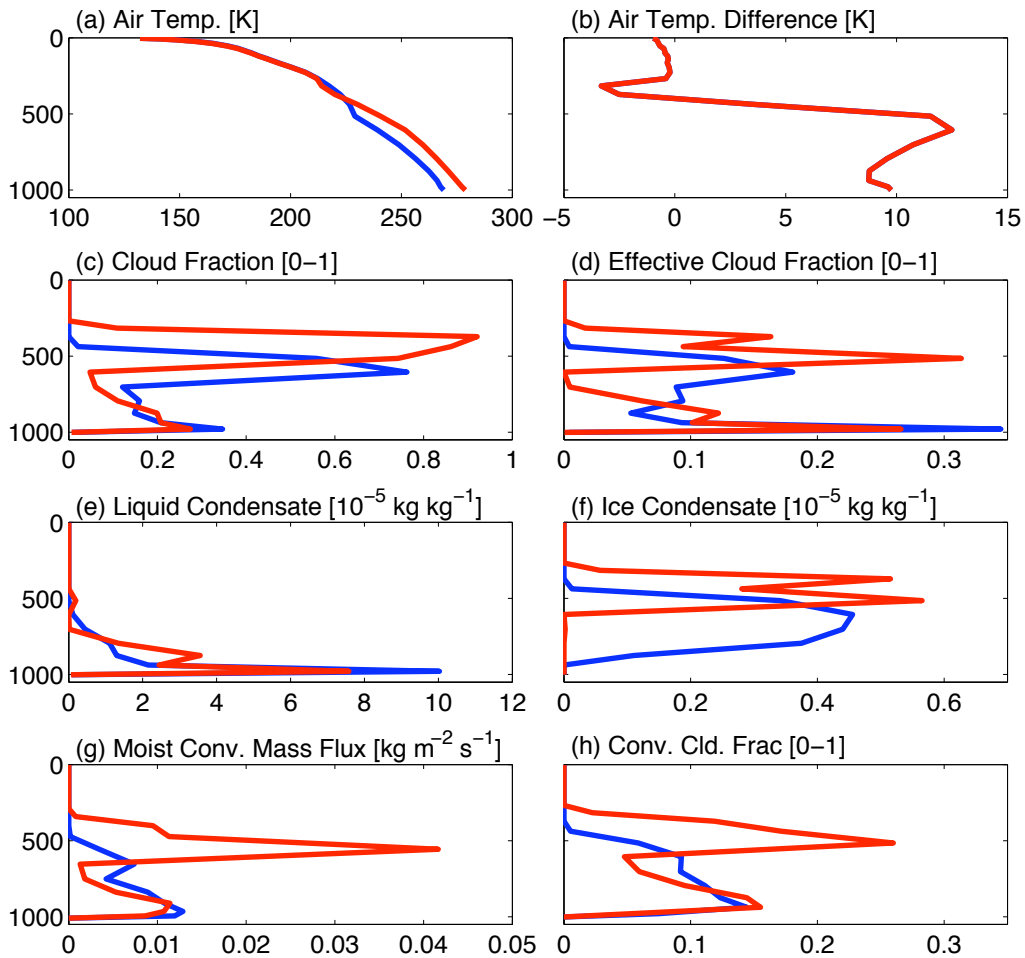
FIGURE 6: Vertical profiles of important SCAM output with zero solar radiation (S=0 W m^{-2}), an atmospheric heat transport (AHT) of 100 W m^{-2}, a net surface heat flux (NSHF) of 70 W m^{-2}, and CO$_2$=2 000 ppm for the warm (red) and cold (blue) states. The effective cloud fraction is the product of the cloud fraction and the cloud emissivity for each layer. The convective cloud fraction is the cloud fraction produced by the convection scheme. The total cloud fraction in a region with convection is often higher than the convective cloud fraction because the model often produces stratiform clouds in these regions as well.

29

List of Tables

TABLE 1: The critical CO_2 concentration (ppm), the lowest CO_2 concentration at which the warm state can exist (the convective cloud feedback can be active), in SCAM as a function of the prescribed atmospheric heat transport (AHT) and net surface heat flux (NSHF). We ran SCAM at every doubling of CO_2 concentration between 250 ppm and 16 000 ppm, as in Figs. 4 and 5. The warm state does not exist at any CO_2 concentration below 16 000 ppm for AHT=90 W m^{-2} and NSHF=60 and 70 W m^{-2}.

	NSHF=60 W m^{-2}	NSHF=70 W m^{-2}	NSHF=80 W m^{-2}
AHT=90 W m^{-2}	-	-	2 000
AHT=100 W m^{-2}	8 000	1 000	250
AHT=110 W m^{-2}	250	250	250

TABLE 2: The maximum temperature difference (°C) between the warm and cold states in SCAM as a function of the prescribed atmospheric heat transport (AHT) and net surface heat flux (NSHF). We ran SCAM at every doubling of CO_2 concentration between 250 ppm and 16 000 ppm, as in Figs. 4 and 5. The warm state does not exist at any CO_2 concentration below 16 000 ppm for AHT=90 W m^{-2} and NSHF=60 and 70 W m^{-2}.

	NSHF=50 W m^{-2}	NSHF=60 W m^{-2}	NSHF=70 W m^{-2}
AHT=90 W m^{-2}	-	-	3.5
AHT=100 W m^{-2}	8.7	8.8	5.2
AHT=110 W m^{-2}	9.8	10.2	3.5